THE JOURNAL OF PHYSICAL CHEMISTRY B

ARTICLE

pubs.acs.org/JPCB

Hierarchical Dynamics of Correlated System−Environment Coherence and Optical Spectroscopy

Kun-Bo Zhu,[†,‡] Rui-Xue Xu,[*,¶,‡] Hou Yu Zhang,[†,‡] Jie Hu,[‡] and Yi Jing Yan[*,¶,‡,†]

[†]State Key Laboratory of Supramolecular Structure and Materials, Jilin University, Changchun 130012, China

[‡]Department of Chemistry, Hong Kong University of Science and Technology, Kowloon, Hong Kong SAR, China

[¶]Hefei National Laboratory for Physical Sciences at the Microscale, University of Science and Technology of China, Hefei, Anhui 230026, China

ABSTRACT: We propose an efficient construction of the hierarchical equations of motion formalism of quantum dissipation on the basis of the Padé spectrum decomposition of the Bose function and the multiple Brownian oscillators decomposition of the environment spectral density. The related hierarchical Liouville space algebra for quantum dissipative mechanics is outlined in relation to the evaluation of nonlinear optical response functions. With the simulated transient pump−probe spectroscopy of model exciton systems, we demonstrate the correlated system−environment coherence by the present nonperturbative and non-Markovian quantum dissipation theory.

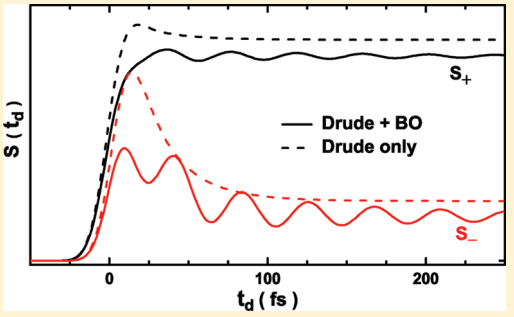

1. INTRODUCTION

Optical spectroscopy using femtosecond tunable laser pulses provides a versatile and powerful tool in exploration and understanding of molecular structures, interactions, and dynamics.[1−3] The ability of extracting complex molecular information from spectroscopic measurements depends generally on a close interplay between theory, simulation, and experiment. Optical response functions, together with their double-sided Feynman pathways contributions, provide a unified treatment of various spectroscopic signals and underlying matter−light interactions.[1−6] Simulations are needed to elucidate the underlying mechanisms via molecular interactions and real-time dynamics. Concerned here is not just a suitable dynamics theory itself but also the efficient numerical propagator for it. The situation becomes extremely challenging in nanostructured functional molecular systems such as excitation energy transfer in biological photosynthesis processes. These systems are often characterized by many-particle interactions, nonperturbative environmental influences, and non-Markovian quantum dissipative dynamics. A full-space or all-atom dynamics approach to optical correlation functions of complex molecular systems goes practically only by certain quasi-/semiclassical treatments.[7−10]

In this work, we exploit the hierarchical equations of motion (HEOM) formalism of quantum dissipation. This approach was originally proposed in 1989 by Tanimura and Kubo for semiclassical dissipation.[11] As a numerically efficient alternative to the path integral influence functional[12,13] and also to an advanced stochastic description of quantum dissipation,[14] the exact HEOM theory[15−19] (including its second quantization[20]) for a general Gaussian dissipation is now established. It has been applied to such processes as electron transfer,[21,22] nonlinear optical spectroscopy,[23−26] and transient quantum transport.[27−29] Apparently, optical response functions defined originally in the full system plus environment composites matter space should now be recast in the reduced hierarchical Liouville space as defined by HEOM.

The dynamics quantities in HEOM are a set of well-defined auxiliary density operators (ADOs) $\{\rho_n(t)\}$. The reduced system density operator of primary interest, defined as the environmental trace of the total density operator $\rho(t) \equiv \mathrm{tr}_B\rho_{\mathrm{tot}}(t)$, is just the zeroth tier one, that is, $\rho(t) \equiv \rho_{n=0}(t)$. ADOs are the reduced system space quantities but contain effectively complete information about the Gaussian statistics of the quantum environment. They resolve not just system−environment coupling strength but also full spectroscopic characteristics of the bath environment, including even those of optically active phonons. The correlated system−environment coherence described by HEOM will be highlighted in this work.

Moreover, an explicit HEOM form goes with the scheme of decomposing the environment correlation function into its multiple memory/frequency components. In a sense, it is an analogy to the choice of the statistical environment basis set for the HEOM construction. The spectrum of the phonon environment correlation function is dictated by the fluctuation−dissipation theorem to be the product of the spectral density and Bose function.[30,31] The conventional HEOM construction involves the Matsubara spectrum decomposition (MSD) for the Bose function.[15−18] However, MSD is notorious for its slow convergence.

Special Issue: Shaul Mukamel Festschrift

Received: January 8, 2011
Revised: March 14, 2011
Published: March 31, 2011

The resulting HEOM is rather expensive and limited largely to simple systems with Drude dissipations. We request the best statistical environment basis set for an efficient HEOM construction and its practical applications. We have shown recently that the Padé spectral decomposition (PSD) is the best sum-over-poles (SOP) scheme for the Bose function.[32] The PSD poles are all purely imaginary and can be accurately evaluated via eigenvalues of a real symmetric matrix.[32] This work will provide further the accurate determination of PSD coefficients via eigenvalue problems. For the environmental spectral density, we adopt the multiple Brownian oscillators (MBO) model.[3−6] It can describe optically actively vibronic coupling via the underdamped Brownian oscillator (BO) mode and also energy fluctuation via strongly overdamped Drude dissipation.

We present the efficient HEOM theory via the PSD-MBO scheme in section 2. Quantum dissipative mechanics via HEOM theory are then outlined in section 3, making contact with the evaluation of linear and nonlinear optical response functions. Numerical demonstrations on vibrational versus electronic coherences are made in section 4 for the transient spectroscopies in the pump−probe scenario of model exciton systems. Finally, we summarize the paper in section 5.

2. HIERARCHICAL THEORY OF QUANTUM DISSIPATION

A. HEOM Formalism. The HEOM has the following compact form[18]

$$\dot{\rho}_{\boldsymbol{n}}(t) = -[\mathrm{i}\mathscr{L}(t) + \gamma_{\boldsymbol{n}} + \delta\mathscr{R}_{\boldsymbol{n}}]\rho_{\boldsymbol{n}}(t) + \rho_{\boldsymbol{n}}^{\{-\}}(t) + \rho_{\boldsymbol{n}}^{\{+\}}(t) \tag{1}$$

It describes not just the reduced system dynamics but also the statistically complete information about the interacting Gaussian environment. The above fact will become evident via the molecular dynamics and optical spectroscopy of model systems studied later in this work. Throughout of the paper, we set $\hbar = 1$ and $\beta = 1/(k_{\mathrm{B}}T)$, with k_{B} being the Boltzmann constant and T the temperature.

The total system−environment composite Hamiltonian in the presence of laser pulsed fields assumes

$$H_{\mathrm{tot}}(t) = H(t) - \sum_a Q_a F_a(t) \tag{2}$$

The reduced system Hamiltonian $H(t)$ in the presence of time-dependent external laser fields enters HEOM (eq 1) via the corresponding Liouvillian, $\mathscr{L}(t)\cdot \equiv [H(t),\cdot]$. The second term on the right-hand-side (rhs) of eq 2 denotes the system−environment coupling $H'(t)$, where Q_a is a system operator, while $F_a(t) \equiv \mathrm{e}^{\mathrm{i}h_{\mathrm{B}}t}F_a\mathrm{e}^{-\mathrm{i}h_{\mathrm{B}}t}$ is a stochastic environment operator and assumes Gaussian statistics. The system operator Q_a is also called the dissipative mode, through which the generalized Langevin force $F_a(t)$ acts on the system. We can always set $\langle F_a(t)\rangle_{\mathrm{B}} \equiv \mathrm{tr}_{\mathrm{B}}\{F_a(t)\mathrm{e}^{-\beta h_{\mathrm{B}}}\}/Z_{\mathrm{B}} = 0$ by defining the reduced system Hamiltonian as $H(t) = \langle H_{\mathrm{tot}}(t)\rangle_{\mathrm{B}}$. The effect of the Gaussian environment on the system is then completely determined by the correlation functions

$$C_{ab}(t) \equiv \langle F_a(t)F_b(0)\rangle_{\mathrm{B}} = \frac{1}{\pi}\int_{-\infty}^{\infty}\mathrm{d}\omega\,\frac{\mathrm{e}^{-\mathrm{i}\omega t}J_{ab}(\omega)}{1-\mathrm{e}^{-\beta\omega}} \tag{3}$$

The second identity is the fluctuation−dissipation theorem.[30,31] It relates the correlation function $C_{ab}(t)$ to spectral density $J_{ab}(\omega)$ that satisfies the positivity, that is, $J_{aa}(\omega)J_{bb}(\omega) \geq |J_{ab}(\omega)|^2$. To illustrate how HEOM depends on the statistical dynamics of the Gaussian environment, we hereafter focus on the single dissipative mode case, that is, $H'(t) = -QF(t)$, and recast eq 3 as

$$C(t) = \frac{1}{\pi}\int_{-\infty}^{\infty}\mathrm{d}\omega\,\frac{\mathrm{e}^{-\mathrm{i}\omega t}J(\omega)}{1-\mathrm{e}^{-\beta\omega}} \approx \sum_{k=1}^{K} c_k\mathrm{e}^{-\gamma_k t} \tag{4}$$

The second identity can be obtained via the Cauchy contour integration technique. It employs certain SOP schemes to decompose both the Bose function and the environmental spectral density. Note that the complex exponents, if they exist, appear in conjugated pairs.

The SOP schemes serve as the stochastic environmental basis set as the exponential expansion of $C(t)$ dictates uniquely the explicit HEOM expressions that resolve the K memory/frequency components as decomposed. The individual ADO is now labeled by $\rho_{\boldsymbol{n}} \equiv \rho_{n_1,\ldots,n_K}$, with $n_k \geq 0$. Its leading contribution is of the n_kth order in the individual exponential component of $C(t)$. We call $\rho_{\boldsymbol{n}}$ an nth-tier ADO, where $n = n_1 + \ldots + n_K$. Its leading contribution is therefore of $(2n)$th-order in the system−environment coupling. The reduced system density operator of primary interest is just the zeroth-tier ADO, $\rho(t) \equiv \rho_{\boldsymbol{0}}(t)$. Note that $\gamma_{n=0} = \rho_{n=0}^{\{-\}} = 0$, as inferred below.

The damping parameter in HEOM (eq 1) collects all relevant exponents[18]

$$\gamma_{\boldsymbol{n}} = \sum_{k=1}^{K} n_k\gamma_k \tag{5}$$

The tier-up/down $\rho_{\boldsymbol{n}}^{\{\pm\}}$ is also additive with respect to each individual real exponent component or pair of complex conjugate exponents components in eq 4. Let $\gamma_{k'} = \gamma_k^*$ to specify a complex conjugate exponents pair, if they exist. It does not imply that $c_{k'} = c_k^*$. Note that $k' = k$ if γ_k is real. Exploiting the standard hierarchical construction algebra,[18] followed by rescaling for numerical filtering,[33] we express the tier-down and tier-up terms, respectively, as

$$\rho_{\boldsymbol{n}}^{\{-\}} = -\mathrm{i}\sum_{k=1}^{K}[n_k^2/|c_kc_{k'}|]^{1/4}(c_kQ\rho_{\boldsymbol{n}_k^-} - c_{k'}^*\rho_{\boldsymbol{n}_k^-}Q) \tag{6}$$

$$\rho_{\boldsymbol{n}}^{\{+\}} = -\mathrm{i}\sum_{k=1}^{K}[(n_k+1)^2|c_kc_{k'}|]^{1/4}[Q,\rho_{\boldsymbol{n}_k^+}] \tag{7}$$

Here, $\rho_{\boldsymbol{n}_k^\pm}$ denotes the associated $(n\pm1)^{\mathrm{th}}$-tier ADO, whose labeling index $\boldsymbol{n}_k^\pm$ differs from $\boldsymbol{n}$ only by changing the specified n_k to $n_k \pm 1$.

In eq 1, $\delta\mathscr{R}_{\boldsymbol{n}}$ is the residue dissipation superoperator, related to $\delta C(t) \equiv C(t) - \sum_{k=1}^{K} c_k\mathrm{e}^{-\gamma_k t}$, the deviation of the finite expansion from the exact environment correlation function $C(t)$ in eq 4. There are two practical treatments of the residue contribution. One is the zero-residue ansatz; $\delta C(t) \approx 0$ and thus $\delta\mathscr{R}_{\boldsymbol{n}} = 0$. Another is the white noise residue (WNR) ansatz; $\delta C(t) \approx 2\Delta\delta(t)$ and consequently $\delta\mathscr{R}_{\boldsymbol{n}}\rho_{\boldsymbol{n}} = \Delta[Q,[Q,\rho_{\boldsymbol{n}}]]$. The applicability of each ansatz can be controlled rather accurately.[22,26]

Beside the statistical basis set that defines the K-space size, HEOM (eq 1) should also be terminated at a sufficiently large tier level L. The number of total ADOs is $\mathscr{N}(L,K) = \sum_{n=0}^{L}(n + K - 1)!/(n!(K-1)!) = (L+K)!/(L!K!)$. This combinatory

dx.doi.org/10.1021/jp2002244 |J. Phys. Chem. B 2011, 115, 5678–5684

law resembles the full configuration interaction in quantum mechanics. With a converged K, the resulting reduced density operator $\rho(t)$ dynamics will be exact at least up the $(2L)$th-order system−environment coupling. Physically, the required L is controlled mainly by the slowest memory component of the environmental correlation function.[17] Efficient HEOM propagators have been proposed, especially the on-the-fly filtering algorithm.[33] It dramatically reduces the effective number of ADOs, so that $\mathcal{N}_{\rm eff} \ll \mathcal{N}(L,K)$, and meanwhile, it also automatically truncates the hierarchy level L.[33]

B. Efficient Sum-over-Poles Schemes. *1. Padé Spectrum Decomposition of the Bose Function.* We have recently proposed PSD be the best SOP scheme for the Bose function.[32] It reads

$$\frac{1}{1-\mathrm{e}^{-\beta\omega}} \approx \frac{1}{\beta\omega}+\frac{1}{2}+\frac{\omega}{\beta}\sum_{k=1}^{N}\frac{2\eta_k}{\omega^2+\breve{\gamma}_k^2} \tag{8}$$

accurate up to the $(4N-1)$th-order in $\beta\omega$. The Padé frequencies $\{\breve{\gamma}_k\}$ and coefficients $\{\eta_k\}$ are all positive.[32] In fact, the summation component of eq 8 amounts to the Padé approximant $P_{N-1}(y)/Q_N(y)$, where $y=(\beta\omega)^2$. The roots of the denominator polynomial $Q_N(y)$ are all negative, given by $\{-\xi_k^2; k=1, ..., N\}$, where $\xi_k \equiv \beta\breve{\gamma}_k$. We have shown that $\{\pm 2/\xi_k\}$ are the eigenvalues of the real symmetric matrix Λ of[32]

$$\Lambda_{mn} = \frac{\delta_{m,n\pm 1}}{\sqrt{(2m+1)(2n+1)}} \qquad m,n=1,...,2N \tag{9}$$

The PSD coefficients $\{\eta_k\}$ in eq 8 can also be accurately evaluated via eigenvalue problems. Using the same algebra of ref 32, we can further show that the roots of numerator $P_{N-1}(y)$ are also all negative. Denote them as $-\zeta_1^2, ..., -\zeta_{N-1}^2$, where $\zeta_j > 0$. Now, remove the last row and column of the matrix Λ and denote the resulting $(2N-1)\times(2N-1)$ matrix as Λ'. Its eigenvalues are shown to be $\pm 2/\zeta_1, ..., \pm 2/\zeta_{N-1}$, and 0. After some elementary algebra, we obtain finally the PSD coefficients of the expression

$$\eta_k = \frac{1}{2}N(2N+3)\prod_{j=1}^{N-1}(\zeta_j^2-\xi_k^2)\Big/\prod_{j=1}^{N}{}'(\xi_j^2-\xi_k^2) \tag{10}$$

The denominator product here runs over all $j \neq k$. We have thus completed the final PSD expression of the Bose function.

Note that the MSD of the Bose function has a similar expression as eq 8 but with the Matsubara frequencies $\breve{\gamma}_k^{\rm MSD} = 2\pi k/\beta$ and coefficients $\eta_k^{\rm MSD}=1$, which are independent of N. In contrast, the PSD poles and coefficients depend generally on N. The accuracy length of PSD versus that of MSD has been analyzed thoroughly.[32] To get a sense about why PSD is remarkably superior over MSN, let us examine

$$\left\{\begin{array}{l}\dfrac{\breve{\gamma}_k}{\breve{\gamma}_k^{\rm MSD}} = 1.000, 1.000, 1.000, 1.003, 1.062, 1.393, 3.486\\[2ex] \dfrac{\eta_k}{\eta_k^{\rm MSD}} = 1.000, 1.000, 1.000, 1.048, 1.761, 5.221, 48.47\end{array}\right\}_{N=7}$$

The exemplified poles and coefficients suggest that PSD be considered as an optimally corrected finite Matsubara expansion. The PSD correction tailors primarily those poles and coefficients near the terminal. By doing that, PSD optimally carries out the resum correction for truncation of the infinite Matsubara series.[32] PSD is actually the best possible SOP expression of eq 8. It supports therefore an optimally efficient HEOM construction.

For an efficient HEOM construction, one can start with the $[N/N+1]$-PSD but exploit only the first N poles for the exponential series expansion, that is

$$\gamma_k = \breve{\gamma}_k \qquad c_k = \frac{2\eta_k}{\mathrm{i}\beta}J(z)\Big|_{z=-\mathrm{i}\breve{\gamma}_k} \qquad k=1, \ ... \ ,N \tag{11}$$

The last pole is included in the residue $\delta C(t)$. The WNR treatment for $\delta C(t) \approx 2\Delta\delta(t)$ will then be carried out with justifications[22,26] to determine the required minimum value of N. The resulting HEOM will be of a WNR form, as described earlier, with $\delta\mathscr{R}_{\boldsymbol{n}}\rho_{\boldsymbol{n}} = \Delta[Q,[Q,\rho_{\boldsymbol{n}}]]$ in eq 1. This approach leads often to an optimal, if not the best, hierarchy construction,[34] in conjunction of the following spectral density decomposition scheme.

2. Multiple Brownian Oscillator Model of the Spectral Density. In contact with molecular reality, we consider for the environmental spectral density a MBO decomposition form, $J(\omega) = \Sigma_j J_j(\omega)$, where[3−6,31]

$$J_j(\omega) = \mathrm{Im}\frac{2\lambda_j\omega_j^2}{\omega_j^2-\omega^2-\mathrm{i}\tilde{\gamma}_j\omega} \tag{12}$$

It can be either underdamped $(\tilde{\gamma}_j/2 < \omega_j)$ or overdamped $(\tilde{\gamma}_j/2 > \omega_j)$. Each Brownian oscillator mode has, in general, two poles, $z=-\mathrm{i}\tilde{\gamma}_j/2 \pm (\omega_j^2-\tilde{\gamma}_j^2/4)^{1/2}$, in the lower-half plane that merge to one second-order pole in the critically damped $(\tilde{\gamma}_j/2=\omega_j)$ case. Thus, each Brownian oscillator contributes two exponential terms to $C(t)$ in eq 4, with the exponents of $\gamma_j^{\pm} \equiv \tilde{\gamma}_j/2 \pm \mathrm{i}(\omega_j^2-\tilde{\gamma}_j^2/4)^{1/2}$ and the coefficients of

$$c_j^{\pm} = \frac{2(z+\mathrm{i}\gamma_j^{\pm})J_j(z)}{\mathrm{i}\ \ (1-\mathrm{e}^{-\beta z})}\Big|_{z=-\mathrm{i}\gamma_j^{\pm}} \tag{13}$$

Note that γ_j^+ and γ_j^- are both real for the overdamped case, while they are the complex conjugate for a underdamped mode.

In the strongly overdamped (Smoluchowski) limit, in which $\tilde{\gamma}_j \gg (\omega,\omega_j)$ but $\gamma_{\rm D} \equiv \omega_j^2/\tilde{\gamma}_j$ is finite, eq 12 recovers the Drude model

$$J_{\rm D}(\omega) = \frac{2\lambda_{\rm D}\gamma_{\rm D}\omega}{\omega^2+\gamma_{\rm D}^2} \tag{14}$$

The Drude mode has only one pole $(z=-\mathrm{i}\gamma_{\rm D})$ in the lower-half plane.

Physically, Drude modes are for solvation coordinates that are diffusive, while Brownian oscillators, especially the underdampled modes, represent intramolecular vibrations. The Drude coupling strength parameter $\lambda_{\rm D}$ defines also the solvation energy if its associated dissipative mode Q stands for the energy difference between two electronic states. On the other hand, the coupling strength of an underdamped Brownian oscillator is often expressed in term of the Huang−Rhys factor, which reads $S_j = \lambda_j/\omega_j$ in the free-oscillator limit.

3. HIERARCHICAL LIOUVILLE SPACE THEORY OF OPTICAL RESPONSE

HEOM (eq 1) that can be recast as $\dot{\boldsymbol{\rho}}(t) = -\hat{\boldsymbol{\Lambda}}(t)\boldsymbol{\rho}(t)$ serves the fundamental formalism for quantum mechanics in dissipative medium. The HEOM generator $\hat{\boldsymbol{\Lambda}}(t)$ is determined by the specific form of eq 1, as described earlier. The HEOM propagator

$\hat{\mathscr{G}}(t,\tau)$ is then given via

$$\boldsymbol{\rho}(t) = \hat{\mathscr{G}}(t,\tau)\boldsymbol{\rho}(\tau) \qquad \text{or}$$
$$\partial_t \hat{\mathscr{G}}(t,\tau) = -\hat{\boldsymbol{\Lambda}}(t)\hat{\mathscr{G}}(t,\tau) \tag{15}$$

In the absence of external driving field where $\hat{\boldsymbol{\Lambda}}(t) = \hat{\boldsymbol{\Lambda}}_s$ is time-independent, the HEOM propagator reduces to $\hat{\mathscr{G}}(t,\tau) = \hat{\mathscr{G}}_s(t-\tau) \equiv \exp[-\hat{\boldsymbol{\Lambda}}_s(t-\tau)]$.

The above expressions are the Schrödinger picture of dissipative dynamics, defined in the linear HEOM space.[35] Each (vector) element $\boldsymbol{\rho} \equiv \{\rho_0, \rho_{n\neq 0}\}$ here consists of the reduced system density operator, $\rho_{n=0} \equiv \rho$, and all other ADOs. Similarly, a dynamics variable A of the reduced system should also be extended to $\boldsymbol{A} \equiv \{A_0, A_{n\neq 0}\}$ in the HEOM space, where $A_0 \equiv A$, while other $\{A_{n\neq 0}\}$ are auxiliary ones. The extended dynamics variable $\boldsymbol{A}$ will be used to define the Heisenberg picture as below. By definition, the expectation value is[35]

$$\overline{A} \equiv \mathrm{tr}(A\rho) \equiv \langle\langle A|\rho\rangle\rangle = \langle\langle \boldsymbol{A}|\boldsymbol{\rho}\rangle\rangle \equiv \sum_{\text{all } \boldsymbol{n}} \langle\langle A_{\boldsymbol{n}}|\rho_{\boldsymbol{n}}\rangle\rangle \tag{16}$$

It defines also the scalar product in the HEOM space. In the absence of an external field after $t = 0$, we have $\boldsymbol{\rho}(t) = \hat{\mathscr{G}}(t)\boldsymbol{\rho}(0)$ and therefore

$$\overline{A}(t) = \langle\langle \boldsymbol{A}|\boldsymbol{\rho}(t)\rangle\rangle = \langle\langle \boldsymbol{A}(t)|\boldsymbol{\rho}(0)\rangle\rangle \tag{17}$$

where $\boldsymbol{A}(t) \equiv \boldsymbol{A}\hat{\mathscr{G}}_s(t)$, with the initial value of $\boldsymbol{A}(0) = \{A_0(0)= A, A_{n\neq 0}(0)=0\} = \boldsymbol{A}$. In other words, the right-action of $\hat{\mathscr{G}}_s(t)$ on system dynamical variables defines the Heisenberg picture in the HEOM space. The corresponding HEOM is then $\dot{\boldsymbol{A}}(t) = -\boldsymbol{A}(t)\hat{\boldsymbol{\Lambda}}_s$, which reads explicitly as (cf. eq 1 with eqs 6 and 7)

$$\begin{aligned}\dot{A}_{\boldsymbol{n}} = & -A_{\boldsymbol{n}}(\mathrm{i}\mathscr{L} + \gamma_{\boldsymbol{n}} + \delta\mathscr{R}_{\boldsymbol{n}}) \\ & - \mathrm{i}\sum_{k=1}^{K} [n_k^2/|c_k c_{k'}|]^{1/4}(c_k A_{\boldsymbol{n}_k^-} Q - c_k^* Q A_{\boldsymbol{n}_k^-}) \\ & - \mathrm{i}\sum_{k=1}^{K} [(n_k+1)^2|c_k c_{k'}|]^{1/4}[A_{\boldsymbol{n}_k^+}, Q]\end{aligned} \tag{18}$$

The right-action of the reduced system Liouvillian $\mathscr{L}$ reads $O\mathscr{L} = [O,H]$, while that of the residue dissipation superoperator $\delta\mathscr{R}_{\boldsymbol{n}}$ is given by $O\delta\mathscr{R}_{\boldsymbol{n}} = \Delta[[O,Q],Q]$ in the WNR limit; compare the comments after eq 11.

To illustrate the general relation between the HEOM space and the full-space formulations, let us consider the correlation function of two system variables, $\langle A(t)B(0)\rangle = \mathrm{Tr}(\mathrm{e}^{\mathrm{i}H_{\mathrm{M}}t}A\mathrm{e}^{-\mathrm{i}H_{\mathrm{M}}t}B\rho_{\mathrm{M}}^{\mathrm{eq}})$. Here, $A(t) = \mathrm{e}^{\mathrm{i}H_{\mathrm{M}}t}A\mathrm{e}^{-\mathrm{i}H_{\mathrm{M}}t} \equiv A\mathscr{G}_{\mathrm{M}}(t)$, the thermal equilibrium density operator is $\rho_{\mathrm{M}}^{\mathrm{eq}} = \mathrm{e}^{-\beta H_{\mathrm{M}}}/\mathrm{Tr}\mathrm{e}^{-\beta H_{\mathrm{M}}}$, and the traces are all defined in the complete system plus environment composite matter space. It is easy to show via the linear response theory that the correlation function can be recast as[35]

$$\begin{aligned}\langle A(t)B(0)\rangle &= \langle\langle A|\mathscr{G}_{\mathrm{M}}(t)\,\vec{\mathscr{B}}\,|\rho_{\mathrm{M}}^{\mathrm{eq}}\rangle\rangle \\ &= \langle\langle \boldsymbol{A}|\hat{\mathscr{G}}_s(t)\,\vec{\mathscr{B}}\,|\boldsymbol{\rho}^{\mathrm{eq}}\rangle\rangle\end{aligned} \tag{19}$$

The first identity remains in the full matter space, with the superoperator $\vec{\mathscr{B}}$ defined via $\vec{\mathscr{B}}\,\rho_{\mathrm{M}} \equiv B\rho_{\mathrm{M}}$. The second identity is in the HEOM space, with $\vec{\mathscr{B}}\,\boldsymbol{\rho} \equiv B\boldsymbol{\rho} = \{B\rho_0, B\rho_{n\neq 0}\}$. Note that $\boldsymbol{\rho}^{\mathrm{eq}} \equiv \{\rho_0^{\mathrm{eq}}, \rho_{n\neq 0}^{\mathrm{eq}}\}$ involves all ADOs initially at thermal equilibrium. It is determined via the stationary solution to HEOM, that is, $\dot{\boldsymbol{\rho}}^{\mathrm{eq}} = -\hat{\boldsymbol{\Lambda}}_s\boldsymbol{\rho}^{\mathrm{eq}} = 0$, in the absence of external fields. The resulting $\{\rho_{n\neq 0}^{\mathrm{eq}} \neq 0\}$ in general accounts for the initial system−environment correlation.

The full space to HEOM space correspondence as exemplified in eq 19 is general and applicable in evaluation of high-order correlation and response functions. Consider, for example, the optical response of the molecular system to a weak probe laser field. The pump-field-dressed response function in the rotating wave approximation is expressed as[36]

$$R_{\pm}(\tau,t) = \mathrm{i}\langle\langle \boldsymbol{D}_{\mp}|\hat{\mathscr{G}}(t+\tau,t)|D_{\pm}\boldsymbol{\rho}(t)\rangle\rangle \tag{20}$$

Here, $D_{\pm}$ is the electronic transition dipole and is related to the exciton creation/annihilation. In the absence of a pump field, $\hat{\mathscr{G}}(t+\tau,t)$ and $\boldsymbol{\rho}(t)$ in eq 20 are replaced by $\hat{\mathscr{G}}_s(\tau)$ and $\boldsymbol{\rho}_{g/e}^{\mathrm{eq}}$, respectively. It results in the conventional two-time correlation function $R_{\pm}^{(1)}(\tau)$, whose Fourier transform is for steady-state (linear) absorption/emission spectroscopy. In general, $R_{\pm}(\tau,t)$ is the absorptive/emissive response of a pump-field-dressed molecular system to a weak probe field at time t. The evaluation of $R_{\pm}(\tau,t)$ can be carried out in the mixed Schrödinger/Heisenberg picture scheme.[36] Both R_+ and R_- are the key quantities in evaluating pump−probe absorption and time−frequency resolved fluorescence spectroscopies.[36] The transient absorption signal to be numerically demonstrated in the coming section is given by

$$\begin{aligned}S(t_{\mathrm{d}}) = & -\mathrm{Im}\int_{-\infty}^{\infty}\mathrm{d}t\int_{0}^{\infty}\mathrm{d}\tau\,\mathrm{e}^{\mathrm{i}\Delta\Omega_{\mathrm{T}}\tau}E_{\mathrm{T}}^{*}(t+\tau)E_{\mathrm{T}}(t) \\ & \times[R_+(\tau,t+t_{\mathrm{d}}) + R_-^{*}(\tau,t+t_{\mathrm{d}})]\end{aligned} \tag{21}$$

Here, t_{d} denotes the probe delay time with respect to the pump pulse field. $E_{\mathrm{T}}(t)$ and $\Delta\Omega_{\mathrm{T}}$ are the slowly varying envelop and the carrier detuning frequency of the probe field, respectively.

4. DEMONSTRATIONS OF CORRELATED SYSTEM−ENVIRONMENT COHERENCE

As mentioned earlier, the ADOs $\{\rho_{\boldsymbol{n}}(t)\} \equiv \boldsymbol{\rho}(t)$ governed by HEOM contain not just the reduced system dynamics but also the full information about a statistically Gaussian environment. The latter can have the underdamped vibration coherence. For illustration, we study the linear absorption coefficient $\alpha(\omega)$ and transient absorption signals $S(t_{\mathrm{d}})$ of some model monomer and dimer exciton systems. The vibrational versus electronic coherence will be demonstrated.

Let us start with a monomer system

$$H_{\mathrm{M}} = h_{\mathrm{g}}|g\rangle\langle g| + (h_{\mathrm{e}} + \omega_{\mathrm{eg}})|e\rangle\langle e| \tag{22}$$

with the phonon environment Hamiltonians

$$\begin{aligned}h_{\mathrm{g}} &= \frac{1}{2}\sum_j \omega_j(p_j^2 + x_j^2) \\ h_{\mathrm{e}} &= \frac{1}{2}\sum_j \omega_j[p_j^2 + (x_j - d_j)^2]\end{aligned} \tag{23}$$

being modeled by a collection of linearly displaced harmonic oscillators. The electronic transition dipoles are $D_+ = \mu|e\rangle\langle g|$ and $D_- = \mu|g\rangle\langle e|$, with μ being treated as a constant. The system is initially in the thermal equilibrium in the electronic ground state $|g\rangle$ manifold. It is therefore convenient to set the bare environment as $h_{\mathrm{B}} = h_{\mathrm{g}}$. It leads to the initial conditions of $\rho_{n=0}(t_0) = |g\rangle\langle g|$ and $\rho_{n\neq 0}(t_0) = 0$ before optical excitation. All

dx.doi.org/10.1021/jp2002244 |J. Phys. Chem. B 2011, 115, 5678–5684

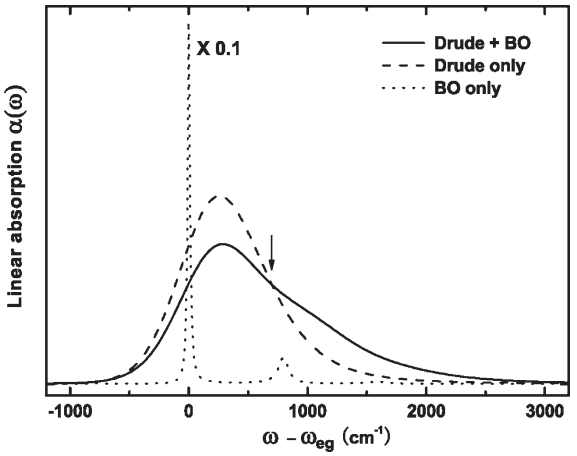

Figure 1. Linear absorption spectrum (arbitrary scale) of the two-level monomer system interacting with either a pure dephasing Drude bath (dash) or an optically active phonon via underdamped Brownian oscillator (dotted) or both (solid).

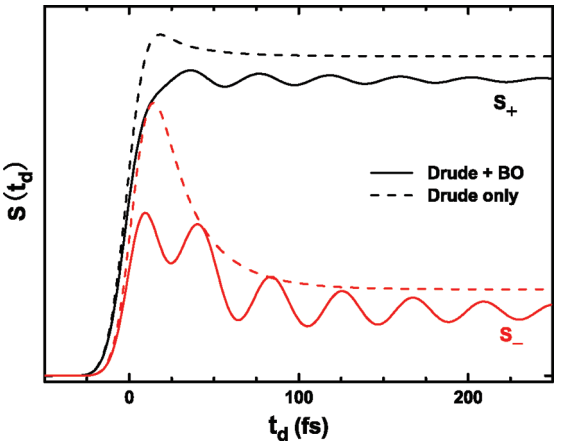

Figure 2. Transient pump−probe difference spectrum for two of the cases in Figure 1. Reported are the individual ground-state hole absorption $S_+(t_d)$ (black curves) and the excited-state particle emission $S_-(t_d)$ (red curves) components of the total signal as functions of the probe delay time t_d. Both the pump and probe are transform-limited 20 fs pulse fields of $\omega_{eg} + 700$ cm^{-1}.

ADOs are 2 × 2 matrices in the two-level systems of study. Equation 22 in the Caldeira−Leggett system−environment coupling form is[30,37,38]

$$H_M = H_0 + \frac{1}{2}\sum_j \omega_j[p_j^2 + (x_j - d_j Q)^2] \qquad (24)$$

with $H_0 = \omega_{eg}|e\rangle\langle e|$ and $Q = |e\rangle\langle e|$. Equation 24 can be recast as $H_M = H_s + h_B + QF$, where $H_s = (\omega_{eg} + \lambda)|e\rangle\langle e|$ and $F = h_e - h_g - \lambda$. The reorganization energy is[31]

$$\lambda = \langle h_e - h_g\rangle_B = \frac{1}{\pi}\int_0^\infty d\omega \frac{J(\omega)}{\omega} \qquad (25)$$

It can be evaluated via the Cauchy contour integration technique and also additive in the MBO model. It is easy to verify that each BO $J_j(\omega)$ in eq 12 contributes with $\lambda = \lambda_j$, which reduces to $\lambda = \lambda_D$ in the Drude limit of eq 14.

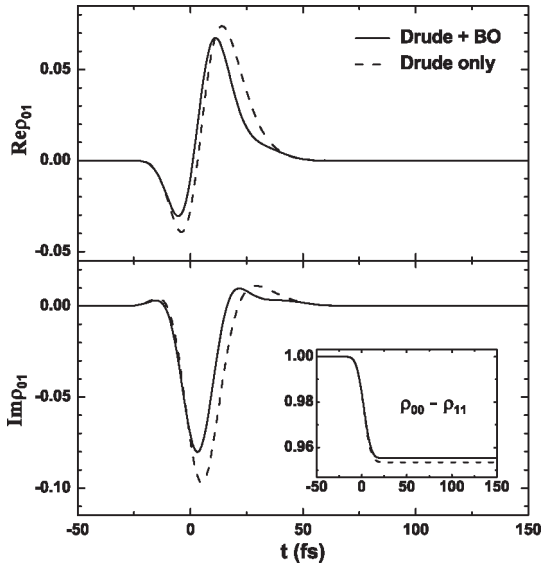

Figure 3. The pump-induced evolution of the reduced two-level system density matrix for the same two cases as those studied in Figure 2. The pump field is a transform-limited 20 fs pulse at $\omega_{eg} + 700$ cm^{-1}. Its temporal center is at $t = 0$.

Figure 1 reports the linear absorption $\alpha(\omega)$ signals of monomer systems at a temperature of $T = 298$ K but with three representing cases of environmental spectral density. The dashed curve is for a Drude mode only, with $\lambda_D = 400$ cm^{-1} and $\gamma_D = 200$ cm^{-1} for $J_D(\omega)$ of eq 14. The dotted curve is only of an underdamped BO (optically active phonon), with the parameters $\omega_{ph} = 800$ cm^{-1}, $\gamma_{ph} = 75$ cm^{-1}, and $\lambda_{ph} = 0.3\omega_{ph}$ (the Huang−Rhys factor is of 0.3) for $J_{ph}(\omega) = J_j(\omega)$ of eq 12 . The solid curve is of both the Drude and BO modes above.

HEOM does contain full information on not only the reduced system, which consists of two levels here, but also its Gaussian environment, including optically active phonon modes. This fact is more transparent by nonlinear spectroscopy, even for the simple transient absorption, as exemplified in Figure 2 for two of the bath environments studied in Figure 1. Reported in Figure 2 are the absorptive $S_+(t_d)$ and emissive $S_-(t_d)$ components of the total pump−probe difference absorption, as given by eq 21, but with the pump-free contribution being removed. They are related to the ground-state hole absorption and the excited-state particle emission, respectively. The pump and probe have the same transform-limited Gaussian form, with the full-width at half-maximum of 20 fs and a central frequency of $\omega_{eg} + 700$ cm^{-1}. The probe is treated pertubatively, with a varying delay time t_d from the pump pulse that centers at the time zero and transfers about 2.2% (2.3%) population onto the excited-state surface. Figure 3 depicts the reduced two-level system density matrix evolution. Apparently, the additional underdamped phonon environment does not alter qualitatively the transient dynamics behavior of the reduced density operator $\rho(t) \equiv \rho_{n=0}(t)$ itself. Thus, the unraveled quantum beats shown by the solid curves in Figure 2 are responsible by not just $\rho_{n=0}(t)$ but also $\rho_{n\neq 0}(t)$. HEOM does describe the correlated system−environment coherence.

Physically optical signal strength reflects the relevant population within a detection window that is defined by the Franck−Condon principle and the given probe frequency. Contrasting to the ground-state hole absorption $S_+(t_d)$, the

dx.doi.org/10.1021/jp2002244 |J. Phys. Chem. B 2011, 115, 5678–5684

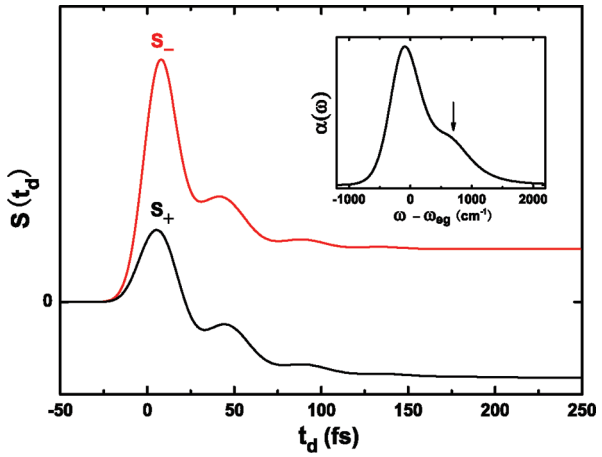

Figure 4. The absorptive $S_+(t_d)$ and emissive $S_-(t_d)$ components of the transient pump−probe difference signal of a dimer system at $T = 298$ K, with Drude on-site energy fluctuation only. The linear absorption spectrum is in the inset.

excited particle emission $S_-(t_d)$ is subject to a dynamics Stokes shift, which is described by the Drude dissipation here. The above simple picture accounts for the observed diffusive features in all curves in Figure 2. Quantum beats shown in the solid curves arise from the additional underdamped BO that is for an optically active phonon. The amplitude of quantum beats in the hole $S_+(t_d)$ versus the particle $S_-(t_d)$ is closely related to that of coherent wavepacket motion on the ground versus the excited surfaces, respectively. Moreover, wavepacket breathing plays roles, especially in the short time behavior of signals, as its period is about half of that for wavepacket center amplitude motion.[4,31,39] The latter is about 42 fs ($\omega_{ph} = 800$ cm^{-1} used here). The first rising piece in $S_+(t_d)$ after the 20 fs pulsed pump field is therefore due to the first contraction of the ground-state hole wavepacket, increasing the population within the homodyne probe detection window. It is well-known that the experimental pump−probe signal consists of the sum of absorptive and emissive contributions. Complementary experiments such as transient fluorescence and two-dimensional spectroscopy[1,2] are needed to separate various dynamics processes.

Turn now to a dimer system, with the dissipative system modes being again for the on-site energy fluctuations, that is, $Q_m = \hat{b}_m^\dagger \hat{b}_m$ ($m = 1,2$), by the diffusive Drude spectral density $J_m(\omega)$ only. Neither cross fluctuation correlation nor vibrational coherence is considered here.The reduce dimer system Hamiltonian reads

$$H(t) = (\varepsilon_1 - \Omega)\hat{b}_1^\dagger \hat{b}_1 + (\varepsilon_2 - \Omega)\hat{b}_2^\dagger \hat{b}_2 + V(\hat{b}_1^\dagger \hat{b}_2 + \hat{b}_2^\dagger \hat{b}_1) + U\hat{b}_1^\dagger \hat{b}_1 \hat{b}_2^\dagger \hat{b}_2 - D_+E(t) - D_-E^*(t) \quad (26)$$

Here, Ω and $E(t)$ are the central frequency and slowly varying envelop of the pump field, respectively. The relevant states are the initial ground state $|0\rangle$, the single-exciton states $|1\rangle$ and $|2\rangle$ on sites, and the double-exciton state $|d\rangle$. The exciton operators in the state representation are $\hat{b}_1 = |0\rangle\langle 1| + |2\rangle\langle d|$ and $\hat{b}_2 = |0\rangle\langle 2| + |1\rangle\langle d|$. The transition dipole operator is $D_- = \mu_{1z}\hat{b}_1 + \mu_{2z}\hat{b}_2 = D_+^\dagger$ along the pump field direction. We set the reorganized on-site energies (cf. eq 24 and the comments there) as $\varepsilon_1 = \varepsilon_2 = \omega_{eg} + \lambda$. Each uncorrelated on-site fluctuation is described by the same Drude bath $J_D(\omega)$, with $\lambda = \lambda_D = 400$ cm^{-1} and $\gamma_D = 200$ cm^{-1}, as adopted earlier for the monomer system. The asymmetry of the dimer arises only from the relative orientation via $\mu_{1z}/\mu_{2z} = 0.35$. The exciton transfer coupling and Coulomb interaction parameters are $V = -300$ cm^{-1} and $U = 100$ cm^{-1}, respectively.

Figure 4 depicts the evaluated $S_+(t_d)$ and $S_-(t_d)$ components of transient pump−probe difference signal of the dimer system, under the same excitation and detection fields as before (20 fs laser pulses at $\omega_{eg} + 700$ cm^{-1}). The monomer counterparts of these spectral components are therefore the dashed curves in Figures 1 and 2. While $S_-(t_d)$ remains as the single-exciton state emission, $S_+(t_d)$ contains now not just the ground-state hole absorption but also the single-exciton state absorption that has the opposite sign of the former two contributions. The quantum beats observed here are of electronic exciton in nature. The dimer absorption depicted in the inset is also red-shifted as it is, in comparison with the monomer absorption.

5. CONCLUDING REMARKS

We have proposed the PSD-MBO scheme to be the choice of statistical environmental basis set for an optimally efficient HEOM construction. We have also demonstrated the HEOM approach to correlated system−environment coherence, together with numerical evaluations on transient pump−probe spectroscopy of some model molecular systems.

We like to emphasis here that HEOM is by far the most numerically tractable formalism for exact quantum dynamics under arbitrary Gaussian environment influence at finite temperature. The explicit HEOM construction depends on the way of decomposing the environmental influence into complex memory components. This is about the statistical environment basis set representation of HEOM quantum dissipation theory. The proposed PSD-MBO scheme is likely the best. We have also verified the established minimum environmental basis set criterions.[22,26] In the present numerical demonstrations, only one PSD pole is sufficient. As the total number of ADOs is concerned, the present HEOM resembles a full configuration interaction formalism in the system−environment coherence space. An efficient filtering algorithm which exists for Drude dissipations[33] needs to be developed further to include the general MBO cases.

AUTHOR INFORMATION

Corresponding Author

*E-mail: rxxu@ustc.edu.cn (R.-X.X.); yyan@ust.hk (Y.J.Y).

ACKNOWLEDGMENT

Support from the NNSF of China (21033008 and 21073169), the National Basic Research Program of China, (2010CB923300 and 2011CB921400), and the Hong Kong RGC (604709) and UGC (AoE/P-04/08-2) is gratefully acknowledged.

REFERENCES

(1) Mukamel, S.; Tanimura, Y.; Hamm, P. Coherent Multidimensional Optical Spectroscopy. *Acc. Chem. Res.* **2009**, *42*; Special Issue.

(2) Abramavicius, D.; Palmieri, B.; Voronine, D. V.; Šanda, F.; Mukamel, S. *Chem. Rev.* **2009**, *109*, 2350–2408.

(3) Mukamel, S. *The Principles of Nonlinear Optical Spectroscopy*; Oxford University Press: New York, 1995.

(4) Yan, Y. J.; Mukamel, S. *J. Chem. Phys.* **1988**, *89*, 5160–5176.

(5) Yan, Y. J.; Mukamel, S. *Phys. Rev. A* **1990**, *41*, 6485–6505.

(6) Yan, Y. J.; Mukamel, S. *J. Chem. Phys.* **1991**, *94*, 179–190.
(7) Thoss, M.; Wang, H.; Miller, W. H. *J. Chem. Phys.* **2001**, *114*, 9220–9235.
(8) Miller, W. H. *J. Chem. Phys.* **2006**, *125*, 132305.
(9) Makri, N. *J. Phys. Chem. A* **2004**, *108*, 806–12.
(10) Martin-Fierro, E.; Pollak, E. *J. Chem. Phys.* **2006**, *125*, 164104.
(11) Tanimura, Y.; Kubo, R. *J. Phys. Soc. Jpn.* **1989**, *58*, 101–114.
(12) Feynman, R. P.; Vernon, F. L., Jr. *Ann. Phys.* **1963**, *24*, 118–173.
(13) Kleinert, H. *Path Integrals in Quantum Mechanics, Statistics, Polymer Physics, and Financial Markets*; World Scientific: Singapore, 2009, 5th ed.
(14) Shao, J. S. *J. Chem. Phys.* **2004**, *120*, 5053–56.
(15) Tanimura, Y. *Phys. Rev. A* **1990**, *41*, 6676–87.
(16) Tanimura, Y. *J. Phys. Soc. Jpn.* **2006**, *75*, 082001.
(17) Xu, R. X.; Cui, P.; Li, X. Q.; Mo, Y.; Yan, Y. J. *J. Chem. Phys.* **2005**, *122*, 041103.
(18) Xu, R. X.; Yan, Y. J. *Phys. Rev. E* **2007**, *75*, 031107.
(19) Yan, Y. A.; Yang, F.; Liu, Y.; Shao, J. S. *Chem. Phys. Lett.* **2004**, *395*, 216–21.
(20) Jin, J. S.; Zheng, X.; Yan, Y. J. *J. Chem. Phys.* **2008**, *128*, 234703.
(21) Shi, Q.; Chen, L. P.; Nan, G. J.; Xu, R. X.; Yan, Y. J. *J. Chem. Phys.* **2009**, *130*, 164518.
(22) Xu, R. X.; Tian, B. L.; Xu, J.; Shi, Q.; Yan, Y. J. *J. Chem. Phys.* **2009**, *131*, 214111.
(23) Ishizaki, A.; Tanimura, Y. *J. Chem. Phys.* **2006**, *125*, 084501.
(24) Ishizaki, A.; Tanimura, Y. *J. Phys. Chem. A* **2007**, *111*, 9269–9276.
(25) Chen, L. P.; Zheng, R. H.; Shi, Q.; Yan, Y. J. *J. Chem. Phys.* **2010**, *132*, 024505.
(26) Tian, B. L.; Ding, J. J.; Xu, R. X.; Yan, Y. J. *J. Chem. Phys.* **2010**, *133*, 114112.
(27) Zheng, X.; Jin, J. S.; Yan, Y. J. *J. Chem. Phys.* **2008**, *129*, 184112.
(28) Zheng, X.; Jin, J. S.; Yan, Y. J. *New J. Phys.* **2008**, *10*, 093016.
(29) Zheng, X.; Jin, J. S.; Welack, S.; Luo, M.; Yan, Y. J. *J. Chem. Phys.* **2009**, *130*, 164708.
(30) Weiss, U. *Quantum Dissipative Systems* 3rd ed.; Series in Modern Condensed Matter Physics; World Scientific: Singapore, 2008; Vol. 13.
(31) Yan, Y. J.; Xu, R. X. *Annu. Rev. Phys. Chem.* **2005**, *56*, 187–219.
(32) Hu, J.; Xu, R. X.; Yan, Y. J. *J. Chem. Phys.* **2010**, *133*, 101106.
(33) Shi, Q.; Chen, L. P.; Nan, G. J.; Xu, R. X.; Yan, Y. J. *J. Chem. Phys.* **2009**, *130*, 084105.
(34) Ishizaki, A.; Tanimura, Y. *J. Phys. Soc. Jpn.* **2005**, *74*, 3131–3134.
(35) Mo, Y.; Xu, R. X.; Cui, P.; Yan, Y. J. *J. Chem. Phys.* **2005**, *122*, 084115.
(36) Shuang, F.; Yang, C.; Yan, Y. J. *J. Chem. Phys.* **2001**, *114*, 3868–79.
(37) (a) Caldeira, A. O.; Leggett, A. J. *Ann. Phys.* **1983**, *149*, 374–456. (b) Caldeira, A. O.; Leggett, A. J. *Ann. Phys.* **1984**, *153*, 445; Erratum.
(38) Caldeira, A. O.; Leggett, A. J. *Physica A* **1983**, *121*, 587–616.
(39) Xu, R. X.; Tian, B. L.; Xu, J.; Yan, Y. J. *J. Chem. Phys.* **2009**, *130*, 074107.